Isolation and characterization of *O*-methyltransferases involved in benzylisoquinoline alkaloids biosynthesis in sacred lotus (*Nelumbo nucifera*)

Ivette M. Menéndez-Perdomo and Peter J. Facchini

SUPPORTING INFORMATION

Figure S1: Visualization and detection of NnOMT1-NnOMT5 recombinant proteins.

Figure S2: *In vitro* 6OMT, 7OMT and 4'OMT activity screening of NnOMTs.

Figure S3: Identification of 7OMT activity of NnOMT5.

Figure S4: Effect of pH and temperature on the catalytic activity of NnOMT1 and NnOMT5.

Figure S5: Steady state enzyme kinetics for NnOMT1 and NnOMT5.

Figure S6: Chromatograms and mass spectra for authentic standards.

Figure S7: NnOMT5 homology model.

Figure S8: Amino acid sequence alignment of NnOMT5 and functionally characterized 7OMTs.

Table S1: Chromatographic and mass spectral data for sacred lotus BIAs detected in this study.

Table S2: NnOMT mRNA sequences used in this study.

Table S3: Amino acid percent-identity matrix among NnOMT candidates and functionally characterized OMTs from BIA-accumulating species.

Table S4: Substrate range for recombinant NnOMT candidates.

Table S5: Alkaloid content in different organs of two sacred lotus varieties.

Table S6: *O*-methyltransferase catalytic activity in different organs of two sacred lotus varieties.

Table S7: OMT transcript levels in different organs of two sacred lotus varieties.

Table S8: Primers used in this study.

Table S9: Amino acid sequence of functionally characterized OMTs involved in BIA biosynthesis in the Ranunculales.

References

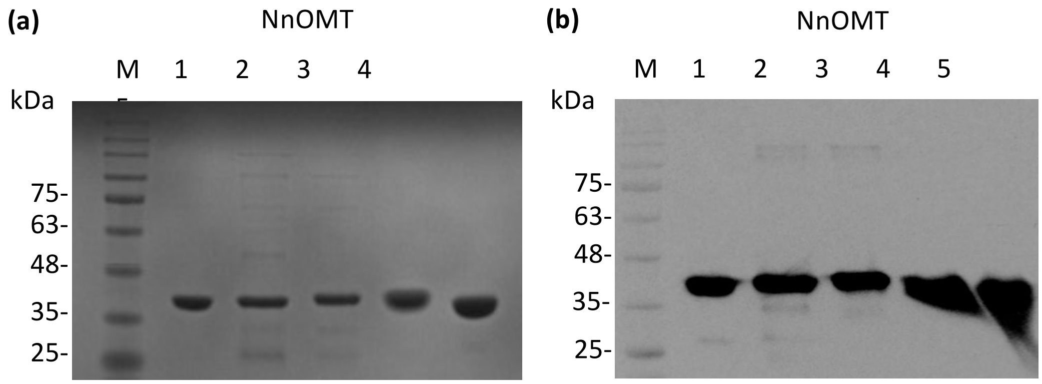

Figure S1: **(a)** Coomassie blue-stained SDS-PAGE and **(b)** Western blot detection of *Nelumbo nucifera* (sacred lotus) *O*-methyltransferase (NnOMT1-5) recombinant His_6-tagged proteins expressed in *Escherichia coli* soluble fraction after cobalt-affinity purification. The molecular weights of marker (M) proteins are shown.

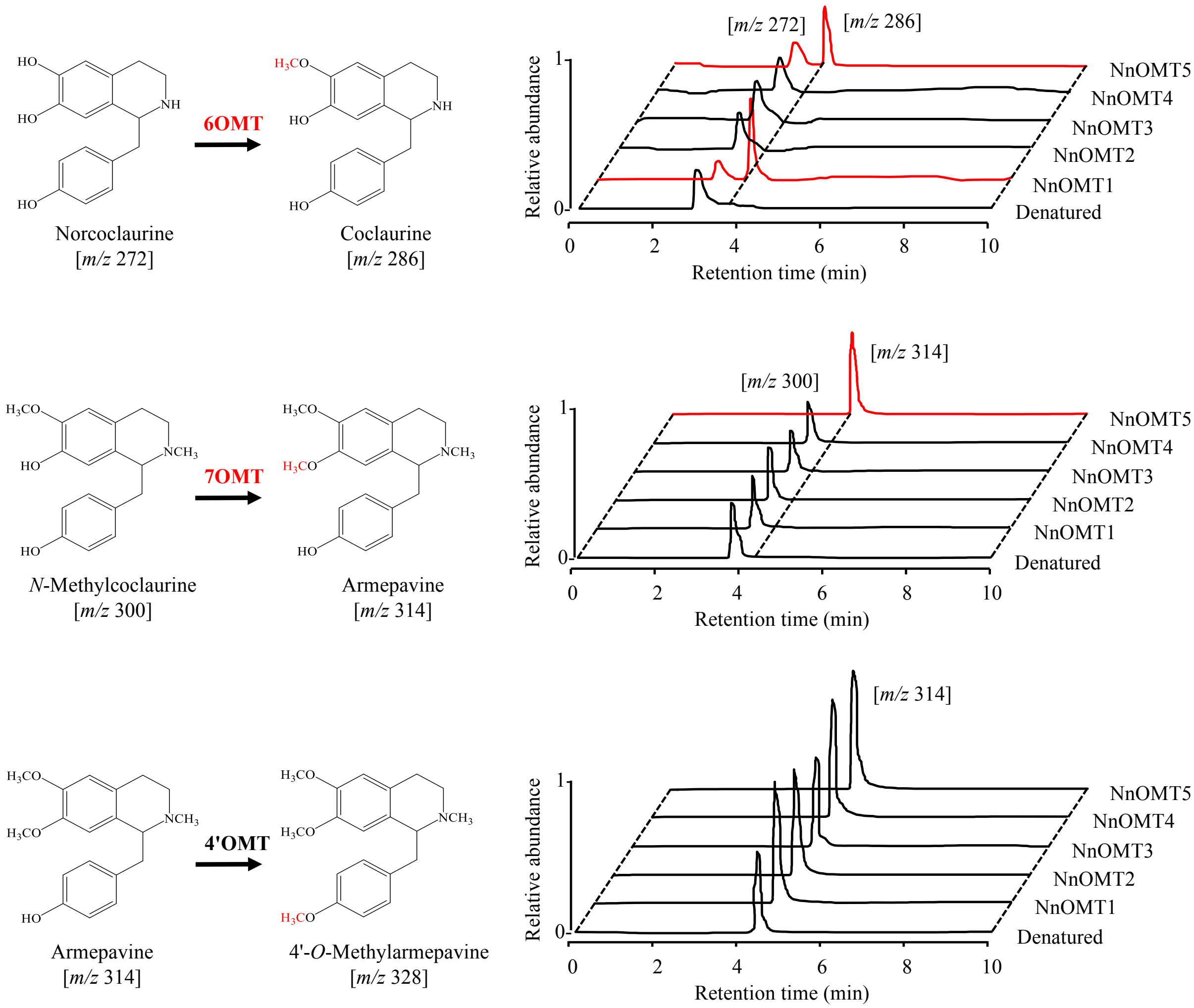

Figure S2: *In vitro* activity screening of recombinant NnOMTs. Expected reactions and chromatograms for selected substrates are shown. Extracted ions of potential reaction products were determined as the addition of 14 Da to the molecular ion of each possible substrate, and chromatographic and mass spectrometric data were compared with available authentic standards (i.e. coclaurine for 6OMT and armepavine for 7OMT reactions, respectively). Double methylations (mass increase in 28 Da) were not detected.

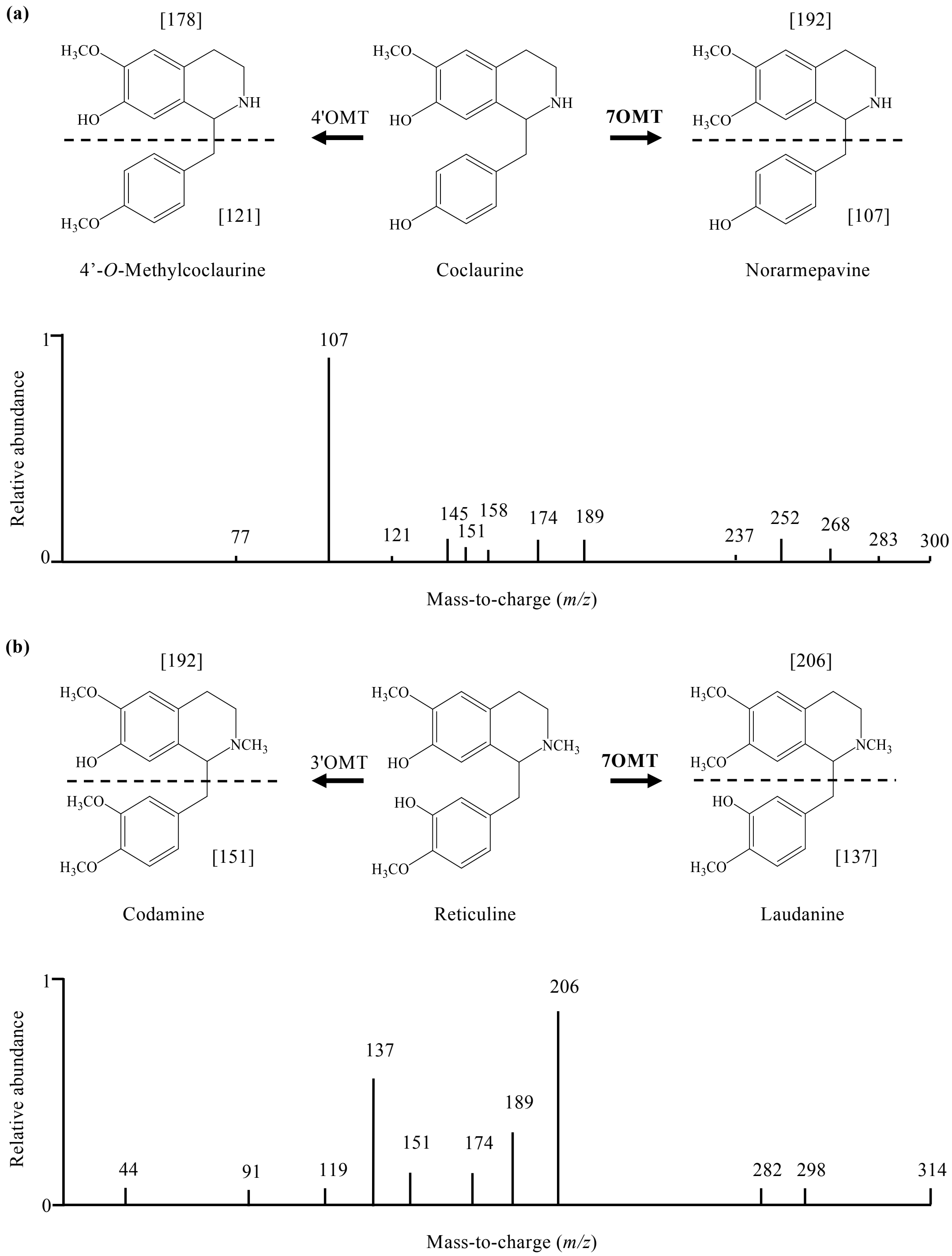

Figure S3: Identification of the *in vitro* reaction products of recombinant NnOMT5. Collision-induced dissociation (CID) analysis of peaks corresponding to the reaction product for **(a)** coclaurine and **(b)** reticuline are shown.

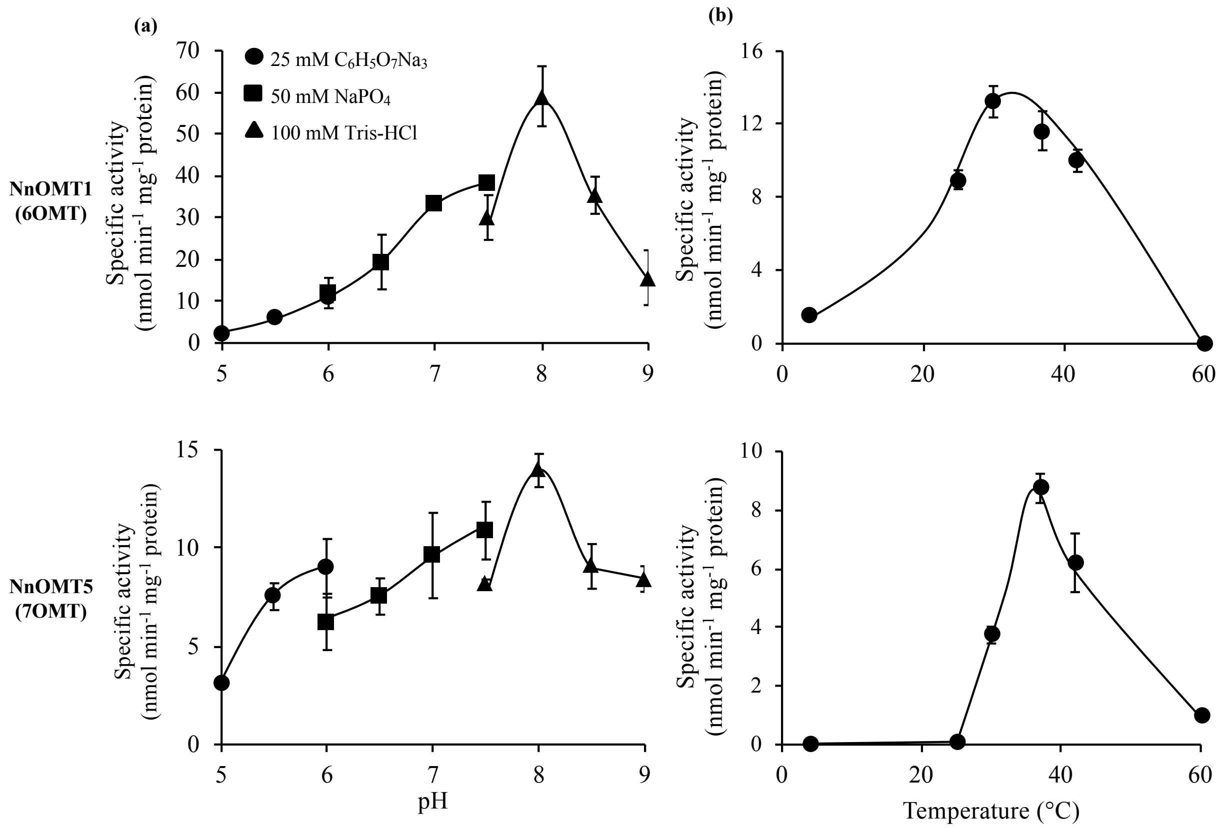

Figure S4: Effect of **(a)** pH and **(b)** temperature on the 6-*O*- or 7-*O*-methylation activity of recombinant NnOMT1 and NnOMT5 using (*R,S*)-norcoclaurine or (*S*)-*N*-methylcoclaurine as substrates, respectively. Values represent the mean ± standard deviation of three independent measurements.

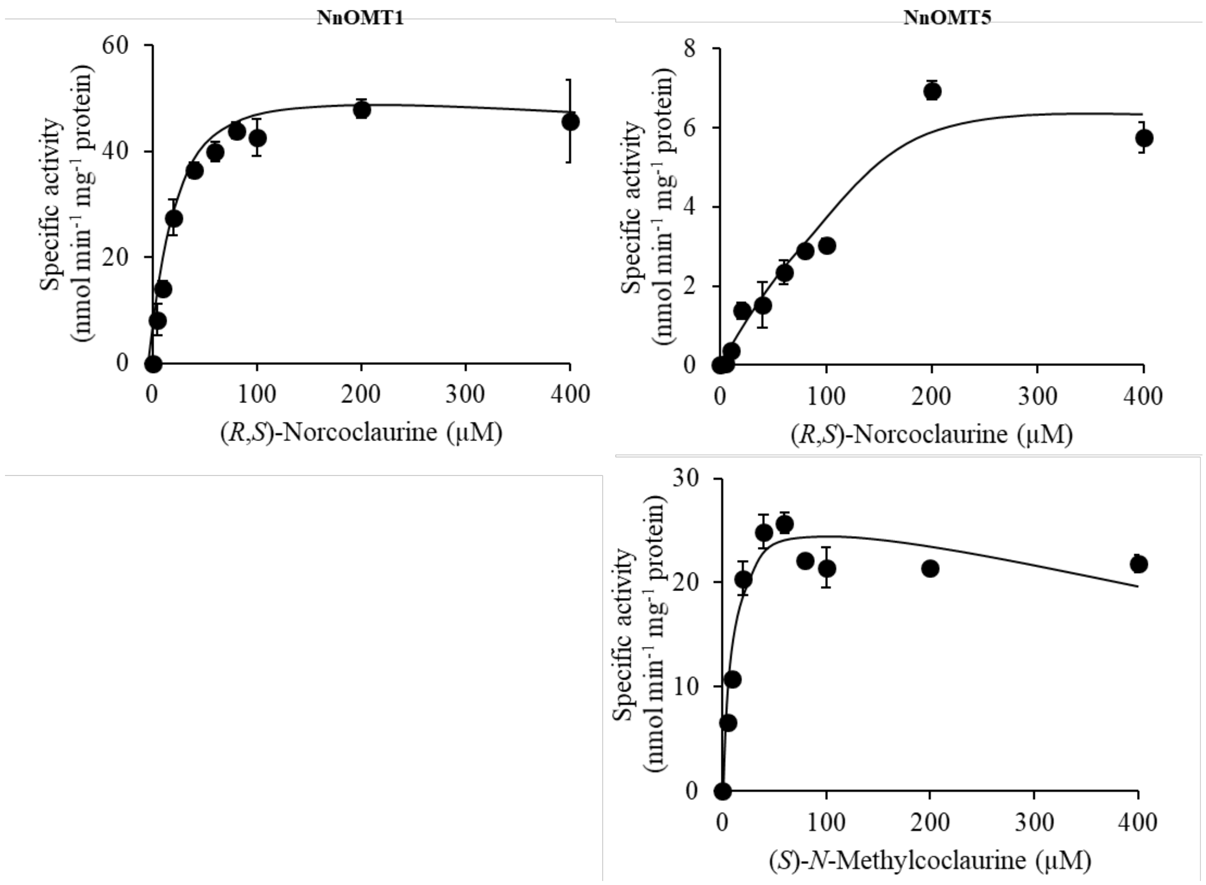

Figure S5: Steady state enzyme kinetics for recombinant NnOMT1 and NnOMT5 using (*R*,*S*)-norcoclaurine and (*S*)-*N*-methylcoclaurine with detection of their corresponding 6OMT and 7OMT activities. Values represent the mean ± standard deviation of three independent measurements.

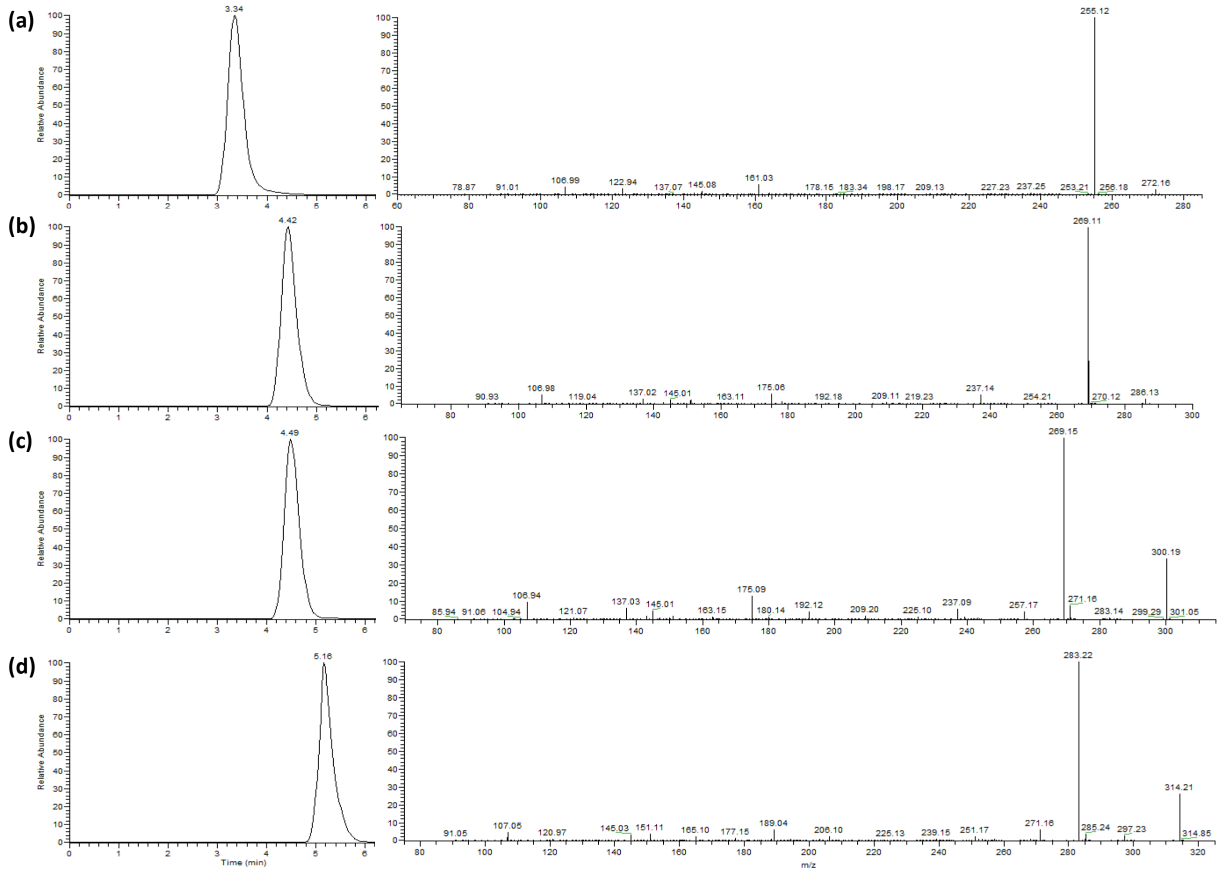

Figure S6: Chromatogram and mass spectrum for authentic standards: **(a)** (*R*,*S*)-norcoclaurine; **(b)** (*S*)-coclaurine; **(c)** (*S*)-*N*-methylcoclaurine; and **(d)** (*R*)-armepavine. Retention times are shown in the chromatograms.

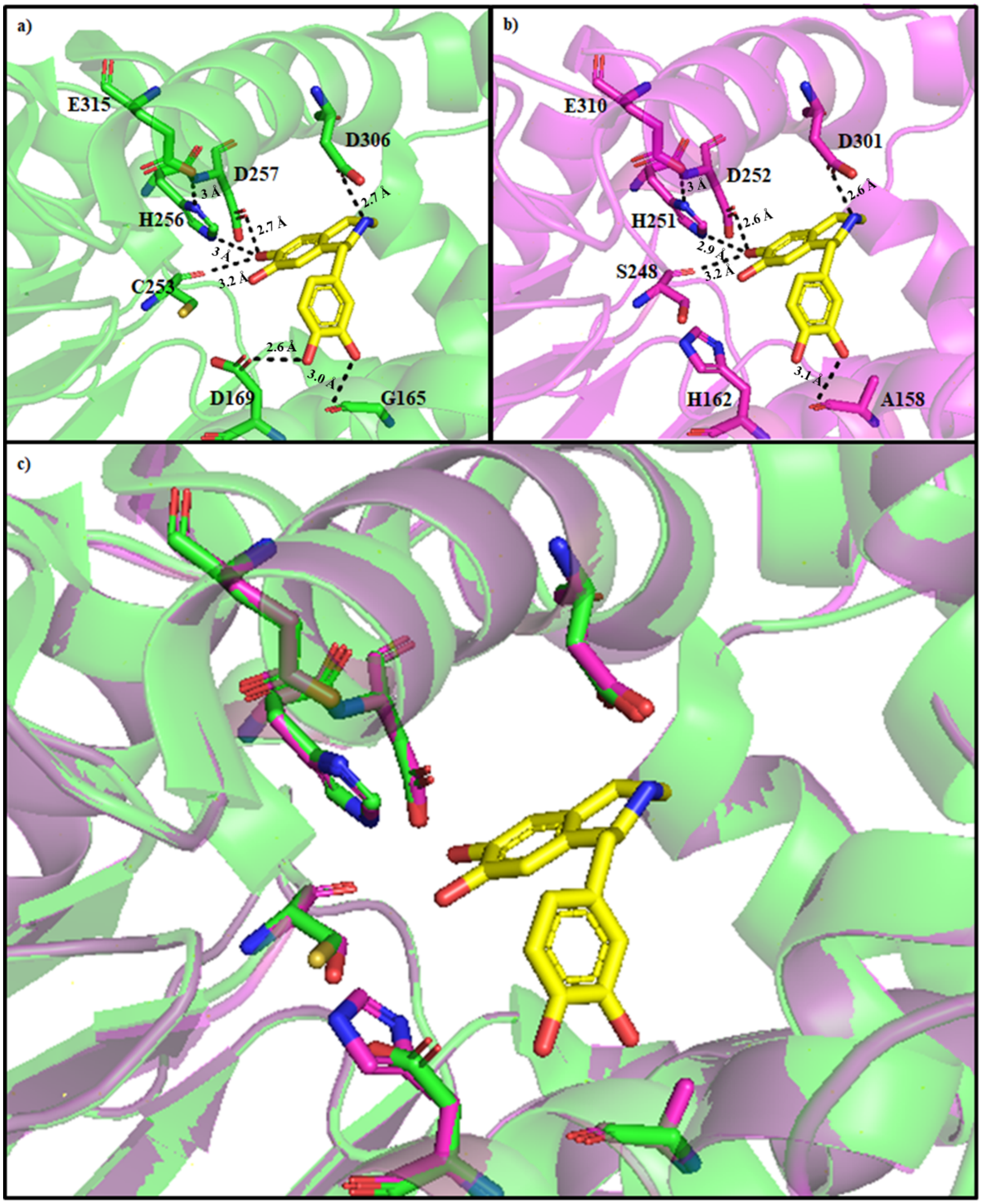

Figure S7: Cartoon representation of **a)** *Thalictrum flavum* 6OMT (Tf6OMT, PDB 5ICE) in green, **b)** *Nelumbo nucifera* OMT5 (NnOMT5) homology model in magenta, and **c)** overlapping Tf6OMT and NnOMT5 structures. Key residues for BIA substrate binding and catalysis are drawn in stick and dot-surface representation to illustrate the shape of the active site around the substrate (*S*)-norlaudanosoline (in yellow). Previously reported interactions between residues in the active site and the substrate (1) are represented by dashed black lines, and distances between atoms are shown in angstroms (Å).

```
NnOMT5     ----MEEDMKAQAQVWKHIYGFVESFTLKCAIELGIADILYEHGQPMTLSELASSIPLP-   55
PsN7OMT    MEVVSQIDQENQAIIWKQIYGFSESLLLKCAVQCEIAETIHNHGTPMSILELAAKLPID-   59
Ps7OMT     -MDTAEERLKGQAEIWEHMFAFVDSMALKCAVELGIPDIINSHGRPVTISEIVDSLKTN-   58
Ct7OMT     ----METILQGQQNITKLLFAFADTMALKCVVELRIADIINSHGLPISLSEIAAGIQSTS   56
Ec7OMT     ---MDEEIILGQADICKYMYGFVDSMTLRCVVELGIPDIIHSHGRPITLTEILNGIPNL-   56

NnOMT5     ----SVSQDGLYRVLRYLVHMKLFDLQVDSD-------GLKKYRLTPASKLLVKNQEKNL   104
PsN7OMT    ---QPVNIDRLYRVMRYLVHQKLFNKEVISTLNGGTVQVTEKYWLAPPAKYLIRGSQQSM   116
Ps7OMT     TPSSSPNIDYLTRIMRLLVHKRLFTSELHQE------SNQLLYNLTRSSKWLLKDSKFNL   112
Ct7OMT     SSSSPPNINYLFRIMRLLVRKGVFSSHAPNQ------NEETLYGLTNSSKWLLRDANFSM   110
Ec7OMT     --SSSFDINYLQGIMTILVRRRVFAVHKFDPKDG-TNLTEIRYGLTPSSKCLLKDSKFNL   113

NnOMT5     ASFVL--LQLYEIDTWNHLSAAVEGTVTPWEKCHGGVDYIEYFKKDSVANQLLSDAMTSH   162
PsN7OMT    VPSVLGIIDEDMFAPWHILKDSLTGECNIFETALGK-SISVYMSENPEMNQISNGAMAFD   175
Ps7OMT     SPLVLWETNPILLKPWQYLGKCAQEKSSPFERAHGC-EIWDLALADPKFNNFLNGAMQCS   171
Ct7OMT     TPIIQALTHHCSMDSFHKLNKCVEEGGYAFAKANGC-EIWEFASMNPEFNRLFNSAMAST   169
Ec7OMT     APFVLLETHPWITDPWNYLGKCVQEGGSGFVKAHGS-DVFKFGSDHPEFFKLFYDGMECS   172

NnOMT5     TSMVTDALVKGCKKAHILDGVGSLIDVGGCTGVAARAIAKWFPSIKCAVFDLPHVVANAP   222
PsN7OMT    SGLVTSHLVNECKSV-FGDEIKTLVDVGGGTGTALRAISKAFPNIKCTLFDLPHVIADSP   234
Ps7OMT     TTTIINEMLLEYKDG-FSGIAGSLVDVGGGTGSIIAEIVKAHPHIQGINFDLPHVVATAA   230
Ct7OMT     SKIAVDAILSGYKNG-FDGLR-SLVDVGGGTGTLIGEIVKAYPHLTGTNFDLPHVVATAP   227
Ec7OMT     TKVLVQVVLDKYQQV-FKDVK-SIVDVGGGTGMMISEIVKNHPHIKGINFDLPHVVAEAP   230

NnOMT5     ECPEVTRIGGDMFVSIPKTDVVFMKSVLHDWGDEDCVKILKKCKEAISEK-GGKAVIVDI   281
PsN7OMT    EIPTITKVSGDMFKSIPSADAIFMKNILHDWNDDECIQILKRCKDVVSA--GGKLIMVEM   292
Ps7OMT     EFPGVKHVGGDMFVDIPEADAVIMKWILHDWSDEDCTIILKNCYRAIRKKKNGKVIIVDC   290
Ct7OMT     EHTGVVHVGGDMFVEIPHADAIILKWILHDWNDEDCVKILKNCHKAIANR-GVKVIIVEI   286
Ec7OMT     DYPGVEHVGGDMFVEIPQADAITMKGILHDWNDDACVKILENCKKAIPK--NGKVIIIDC   288

NnOMT5     VMDVESSPNEFTGARLGMEMDMLVA-VGGKERSEKEWHKLFKEAGYSGYKITPIV---AI   337
PsN7OMT    VLDED-SFHPYSKLRLTSDIDMMVN-NGGKERTEKEWEKLFDAAGFASCKFTQMSVGFAA   350
Ps7OMT     VLRPD-GNDLFDKMGLIFDVLMMAHTTAGKERTEAEWKILLNNAGFPRYNVIRTP---AF   346
Ct7OMT     VLQPD-GVAPLDETRLIFDLSMIAHSSGGKERTETEWEKLLRDGGFSRHRIIQIP---DV   342
Ec7OMT     VLNPD-GDDLFDDIKVVSDLGMRVHCSDGKERTEAEWEKLLKKGGFPRYKITHVV---TV   344

NnOMT5     ESIIEVFP-    345
PsN7OMT    QSIIEVY--    357
Ps7OMT     PCIIEAFPE    355
Ct7OMT     TSIIEAYP-    350
Ec7OMT     QSMIEAYPE    353
```

Figure S8: Amino acid sequence alignment of NnOMT5 and functionally characterized 7-*O*-methyltransferases (7OMTs) from BIA-accumulating species. Fully conserved residues are shaded in black, whereas those shared by NnOMT5 and 7OMTs are shaded in grey. Ct, *Coptis teeta*; Ec, *Eschscholzia californica;* Nn, *Nelumbo nucifera*; Ps, *Papaver somniferum*.

Table S1: Chromatographic and mass spectral data for sacred lotus BIAs detected in this study. AS, authentic standard.

Class	Alkaloid	Formula (+ H)	*m/z* $[M + H]^+$	Rt (min)	Product ions m/z (relative abundance, %)	Reference CID
1-Benzylisoquinoline	Norcoclaurine	$C_{16}H_{18}NO_3$	272.12812	3.3	272(4); 255(100); 161(6); 123(4); 107(4)	AS
	Coclaurine	$C_{17}H_{20}NO_3$	286.14377	4.4	286(3); 269(100); 237(6); 209(2); 175(6); 145(3); 137(3); 107(6)	AS
	N-Methylcoclaurine	$C_{18}H_{22}NO_3$	300.15942	4.4	300(34); 269(100); 237(6); 209(2); 175(13); 145(5); 137(2); 107(10)	AS
	Norarmepavine	$C_{18}H_{22}NO_3$	300.15942	5.3	300(8); 283(100); 268(7); 189(4); 107(4)	(2)
	N-Methylisococlaurine	$C_{18}H_{22}NO_3$	300.15942	5.5	300(100); 269(24); 237(4); 192(12); 175(4); 145(6); 107(8)	(3)
	Armepavine	$C_{19}H_{24}NO_3$	314.17507	5.2	314(26); 283(100); 252(2); 206(2); 190(7); 151(4); 145(4); 107(5)	AS
Aporphine	Anonaine	$C_{17}H_{16}NO_2$	266.11756	8.2	266(1); 249(100)	(4)
	Roemerine	$C_{18}H_{18}NO_2$	280.13321	8.6	280(1); 249(100)	(5)
	N-Nornuciferine	$C_{18}H_{20}NO_2$	282.14886	6.2	282(2); 251(100); 219(54)	(5)
	O-Nornuciferine	$C_{18}H_{20}NO_2$	282.14886	8.0	282(1); 265(100)	(5)
	Nuciferine	$C_{19}H_{22}NO_2$	296.16451	8.4	296(1); 265(100); 250(4)	(3)
Pro-aporphine	Pronuciferine	$C_{19}H_{22}NO_3$	312.15942	4.8	312(62); 283(24); 269(100); 254(4); 238(2); 206 (62); 177(4)	(3)
Bisbenzylisoquinoline	Nelumboferine	$C_{36}H_{41}N_2O_6$	597.29591	5.3	597(100); 566(3); 475(5); 192(12)	(3)
	Liensinine	$C_{37}H_{43}N_2O_6$	611.31156	6.0	611(100); 580(6); 568(6); 489(8); 206(20)	(3)
	Isoliensinine	$C_{37}H_{43}N_2O_6$	611.31156	6.4	611(100); 580(6); 568(4); 475(12) 192(20)	(3)
	Neferine	$C_{38}H_{45}N_2O_6$	625.32721	7.4	625(100); 594(8); 582(4); 503(6); 489(7); 206(8)	(3)

Table S2: *Nelumbo nucifera* OMT mRNA sequences used in this study. The start and stop codons are highlighted in green and red, respectively. GenBank accession numbers are indicated in parentheses.

Gene (Accession)	**mRNA sequence (5'-3')**
NnOMT1 (XM_010245752)	GCACTTAGCACCTGAGTGACAGAAAGAGCTCTAATTAAGTTTAGTAATTTATCTCACTCAGGGCACCGGCT TTTGAGTTTACGAGGGGCATAGAATAGAGAGGAGAATGGAAATTCAGAAGGAAGGTCAAGCAGCGGCGGC TAAAATCTGGAAATTCGTTTATGGCTTTGCCGACTGTTTAGTCCTCCGATGTGCCATTGACCTCGGAATTGC AGACATAATCCATAAGCAGGGAGAACCCTTGACGCTCTCTGAACTGGGGGCTCAAATTCCTGTGCAACCGG TCAACACCGATCACTTGCACAGGTTAATGCGTTACTTGGTGCACATGAAGATCTTCACCAAGGAAACCCTA GATGGCGAAGCACGATATGGGCTGGCTCCACCGGCTAAGTTCATTGTAAAAGGGTGGGACAAGAGCATAG TGTCAATCATATTAGTGGTCACCGACAAGGATTTCATGGCACCCTGGCACTGCCTCAAGGATAGCTTGTGC GGCGAGGGGACAGCTTTTGAGAAGGCGTTAGGGAGGAGCATATGGACATACATGGCTGATCATCCGGAGA AGAATAAGCTCTTCAATGAAGGAATGGCTTGTGATACCAAACTCCTCATATCAGCCTTGGTTCAAGACTGC AAGGATTTATTCCAAGGAATAATGTCGTTGGTGGATGTTGGTGGAGGCACTGGAACTGCCATGAGAGCCAT TGCCAAGGCCTTTCCCCACCTAAAATGTACAATTTATGATCTACCTCATGTCATTGCCGACTCCCCTGATTA CCCTGAGGTCGACCGGATTGCAGGCGACATGTTCAAACACATTCCTAGTGCCGATGCCATCTTATTGAAGT GCATCCTCCATGACTGGGATGATGGTGAATGCATTGAAATTCTAAAGCGATGCAAGGAATCAGTGCCTAGA GAGGGTGGAAAAGTTATCATCGTCGACATAGTAGTAGATTTGGAATCTAAGCATCCCTTAACAAAGACTAG ACTAAGCTTGGATTTGGACATGATGGTCACCACTGGAGGAAAAGAGAGGACTGAGGCAGAATGGAAGAAG CTTTTGAATGCTGCAGGGTTCCCTGTATTTAAGATTACACATATATCTGCCGTTCAATCTGTAATTGTGGCCT ATCCTTATTAGCCTTTTCTCTCTCTCTCCCCAGGTCCTAGCTACGTCTTCTTCTTCAATACTAATAATATTTTA TTTTTGGTCGGTTATATATTAGTGTCATAGGATGGGTTCAAGTCTAAGGGCCTGTTCGTTTGCTCTCAAGTC ATCTGTATGTGTAATAATTACATTAAGAGGTATATTGGTATTGGTGAACC
NnOMT2 (XM_010249599)	TGTAAACATTAAGATGGAAGGCTGTGTCTTGACTACTTGCATTTGCACTTGTCCCTGAGTGAGAGAAAGAG AGAGAGAGCTCTAATTAAGTTCCGTAATTTATCTCGTTCAGGTTACCGGCTTCTGAGTTCAAGAGGGACCTA GAGAGGAGAATGGAAATTCCGAAGGAAGTTCAAGCTGACGAGGTTGAAATCTGGAAATTCGGATATGACT TTGCCGACACTTTAGTCCTCCGATGTGCCATTGAGTTCGGTATTGCAGACATAATCCATAAGCAGGGAGAA CCCTTGACGCTCTTTGAACTGGGGGCTCAAATTCCTGTGCAACCAGTCAACACCGATCACTTGCACAGGTTA ATGCGTTACATGGTGCACATGAAGATCTTCACCAAGGAAACCCTAGGTGGCGAAGAACRATATGGGCTATC TCCACACGGTAAGTTCCTTGTAAAAGGGTGGGACAAGAGCATGGCGTCAGCCATATTAGCGATCACTGACG AGGATTTCTTTGCACCCTGGCACTGTCTCAAGGATGTCTTGGCCGGCGAGGGGACAGCTTTTGAGAAGGCG TTAGGCAAGAGCATATGGGCATACGTGGCTGATCATCCGGAGAAGAATAAACTCTTCAATGAAGTAATGGC TTGTGATACCAGTTTCATCACATCAGTCTTGATTCAAGACTGTAAGGATGTATTCCAAGGAATAAAGTCGGT GGTGGATGTTGGTGGAGGCACTGGAACTGCCATGAGAGACATTGCCAAGGCCTTTCCCCACCTAAAATGTA CAATTTATGATCTACCTCATGTCATTGCCGACTCACCTGATTACCCTGAGGTCGACCGGATTGCAGGCGACA TGTTCAAACACATTCCTAGTGCCGATGCCATCTTATTGAAGTGGATCCTCCATGATTGGGATGATGGTGAAT GTATTGAAATTCTAAAGCGATGCAAGGAATCAGTGCCTAGAGAGGGTGGAAAAGTTATCATCGTCGACATA GTACTAGATCCGGAATCTAAGGATCCCTTAACAAAGGCTAGATTAAGGTTGGATTTGGACATGATGGTCTA CACTGGAGGAAAAGAGAGGAGTGAGGCAGAATGGAAGAAGCTTTTGAATGCTGCAGGGTTCCCTGGATAT AAGATTTTACATGTAGCTGCCGTTCAATCTGTAATTATGGCCTATCCTTATTAGCCTTCTCTCTCTCTCCCCC CCCCCCGGTCCAGCTACTTGTCTTCTTCTTCAGTATTAATAATATTTACTTTTTGTTAGGTTGCACATATATT AGTGTCATAGGATGGGTTCAAGTCTAAGAATGACAATTTTATTAAAGAAAAAAATACCATAGATAGGTTAG GTCTGTATTCAGTTCCTTCTTCCACATAGCTGCGACTAACATTGGATAATGGCTTTCTTGACTATCCATTATC ATATCAATCCATACAATTCCCACTACCTATTACCAACTCCTACCCCTCATCATTCTGTGAGATTGACCATTGT GAGTTTTGATTTACCAACGCTGAATGATTTTCTTGAAAATTTTACTCAATAAAAAAATGGATCATATTAATT ACTATATTTATTTTTGGCATTTTGGTTAAGGTTGTCAAATGGGTCAGGCAGACCCTACAGACCCAAACTGAA TCTACACAATTATAT
NnOMT3 (XM_010249600)	CGTGACTACTTGCCCTAGCATTTGTACCTGAGTGAGAGACAGAGAGAGATAGAGCTCTAATTAAGTTGAGT AATTTATCTTATTCAGGGCACCGGCTTTTGAGTTAAGGAGGGGCATAGAGAGGATAATGGAAATTCAGAAG GAAGTTCAAGCAGCCGACGTTGAAATCAGGAAATTCGGTTATGGCTTTGCCGACATTTTAGTCATCCGATG TGCCATTCAGCTCGGAATTGCAGACATAATCCATAAGCAGGGGGAACCCTTGACGCTCTCTGAACTGGAGG CTCAAATTCCTGTGAAACCGGTCAACACCGATCACTTGCACAGGTTAATGCGTTACATGGTGCACATGAAG ATCTTCACCAAGGAAACCCCTGATGGCGAAGAACGATATGGGCTGGCTCCACTGGGTAAGTTCCTTGTAAA TGGGTGGGACAGGAACATGGTGTCAGCCATATTAGCGGTCACTGACAAGGATTTCATGGTACCCTGGTACC GTCTCAAGGATAGCTTGGTCGGCGAGGGGACAGCTTTTGAGAAGGCGTTAGGGAAGACCATATGCGAATG CATGGCTGATCATCCGGAGAAGAAAAAGCCCTTCAATGAAGCAATGGCTTGTGATACGACCAGGCTCCTCA CATCAGCCTTGATTCAAGACTGCAAGGATTTATTCCAAGGAATAATGTCGTTGGTGGATGTTGGTGGAGGC ACTGGAACTGCCATGAGAGACATTGCCAAGACCTTTCCCCACCTAAAATGTACAATTTATGATCTACCTCAT GTCATTGCCGACTCCCCGGATTACCCTGAGGTCGACCGGATTGCAGGCAACATGTTCAAACACATTCCTAG TGCCGATGGCATCTTGTTGAAGTGCATCCTCCATGACTTGGGTGACCGTCAATGCATTGAAATTCTACAGCG ATGCAAAGAATCAGTGCCTAGAGAGGGTGGAAAAGTTATCATCGTCGACATAGTACTAGATCCGGAATCTA CGGATCCCTTAACAAAGGCCAGATTAAGGTTGGATTTGGACATGATGGTCTACACTGGAGGAAAAGAGAG GAGTGAGGCAGAATGGAAGAAGCTTTTGAATGCTGCAGGGTTCCCTCGATATAAGATTTTACATATAGCTG CCGTTCAATCTGTAATTGAGGCCTATCCTTATTAG
NnOMT4	ATGTAGTCTACTACATTGGAGACCTCCTCCTATCAGACTGAACTGTAAACATTCAAAGGGAACACCGTGAC TACTTGCACTTGTACCTGAGAGAGAGAGAAAAAAGAAAGAGAGGCATGCAGGCATAGAGTAGAGATAGG

(XM_010273389)	AGAATGGAAAATCAGAAGGAAGTTCAAGCAGCCGAGGCTAAAATCTGGAATTTCGTCTATGGCTTTGCCGA CACTTTAGTCCTCCGATGTGCCATTGAGCTGGGTATTGCAGACATAATCCATAAGCAGGGAGAACCCTTGA CGCTCTCTGAACTGGGGGCTCAAATTCCTCTGAAGTCGGTCAACACCGACCACTTGCACAGGTTAATGCGTT ACTTGGTGCACATGAAGCTCTTCACCAAGGAAACCCTAGATGGCGAAGCTCGATATGGGCTGGCTCCACCG GCTAAGTTGCTTGTAAAATGGTGGGAGGACAAGGGCTTGGCGTCAATCATATTTGGGATCACTGACAAGGA TTTCATAGCACCCTGGCACCATCTCAAGGATAGCTTGGCCGGCGATGGCGAGGAGACAACTTTTGAGAAGG TGTTAGGGAAGAGCATATCGACATACATGGCTGATCATCTGGAGAAGAGTATGTTGTTCAATGAATCAATG GTTCATGATACCAGGCTCTTCACATCAGTCTTGATTCAAGACTTCAAGGATGTATTCCAAGGAATTAAGTCG TTGGTGGATGTTGGTGGAGGCTCTGGAACTGACATGGGAGCCATTGCCAAGGCCTTTCCCCACCTAAAATG TACAATTTATGGTCTACCTCATGTCATTGCCGACTCCCCTGATTACCCTGAGGTCGACCGGATTTCAGGCGA CATGTTCAAACACATTCCCAGTGCCGATGCCATCTTATTGAAGTGCATCCTCCATTACTGGGGTGATGGTCA ATGCATTGAAATTCTAAAGAGATGCAAAGAATCAGTGCCTAGAGAGGGTGGAATAGTTATCATCGCCGAC GCAGTAGTAGATTTGGAATCTAAGCATCCCTACTTAACAAAAACTTTACTAAGCACGGATTTGGACATGAT GCTCAACACTGGAGGAAAAGAGAGGACTGAGGCAGAATGGAAGAAGCTTTTTAATGCTGCAGGGTTCCCT GCATATAAGATTACACATGTAGCTGACGTTGAGTACTCTGTAATTGAGGCCTATCCTTATTAGCCTCCCCCC TCCCCCGGTCCAGCAACTTGTCTTCTTCTTCTTCAGTACTAATAATATTTAGCTTTTGTTTGGTTGCATATAT ATTAGTGTATGGGATGGGTTCAAGGCTCACGATGACCATTCCTTTTTCCACA
NnOMT5 (XM_010277761)	CTCCTGCTGGTCTTAGCGGAGCCACAAATCAGTGGTCGACCAGCTCTATAAAAGAAATTCACTGCGTTTGC CAAGAGGCCAATTCGATCGATCACTAAGCTTTTGAGAGAAAGAGAGAAAGATTGAGGCGGACGCCATGGA GGAGGACATGAAAGCTCAAGCCCAAGTGTGGAAACACATATACGGCTTCGTCGAGTCATTCACTCTCAAAT GCGCGATCGAACTCGGGATCGCGGACATACTCTACGAACATGGTCAGCCCATGACTCTCTCCGAGTTAGCC TCCTCCATCCCTCTTCCCTCTGTCAGCCAAGACGGATTGTACAGGGTGTTGCGTTACCTCGTGCACATGAAA CTCTTCGACCTGCAGGTCGATTCCGACGGGTTAAAGAAGTACCGGCTCACTCCCGCGTCCAAGCTCTTGGTC AAAAACCAGGAGAAGAACCTGGCATCCTTCGTTCTCCTGCAATTGTACGAGATAGACACTTGGAACCACCT AAGTGCCGCAGTGGAAGGTACCGTGACACCCTGGGAGAAGTGTCACGGCGGCGTGGACTACATAGAGTAC TTTAAGAAGGACTCGGTGGCGAATCAGTTGTTGAGCGACGCGATGACGAGTCACACGAGTATGGTGACGG ACGCGCTGGTGAAGGGCTGCAAGAAGGCGCACATCCTTGATGGAGTAGGGTCCCTAATTGACGTGGGCGG GTGTACTGGGGTGGCTGCTAGAGCCATCGCTAAGTGGTTCCCCAGTATAAAATGTGCGGTGTTTGATCTGCC CCACGTAGTAGCCAACGCGCCCGAGTGCCCCGAGGTGACTCGGATCGGAGGCGATATGTTCGTATCAATTC CGAAAACGGATGTGGTGTTCATGAAGTCGGTGTTACACGACTGGGGAGACGAGGACTGCGTAAAGATTCT GAAGAAATGCAAGGAGGCGATATCGGAGAAAGGAGGAAAAGCAGTGATCGTGGATATTGTAATGGATGTG GAATCATCGCCGAATGAGTTCACTGGTGCAAGACTGGGGATGGAGATGGACATGCTGGTCGCAGTGGGTG GTAAAGAGAGAAGTGAAAAGGAGTGGCATAAACTCTTCAAGGAAGCGGGTTACAGCGGGTACAAGATAAC ACCCATCGTTGCAATCGAATCAATTATAGAAGTGTTCCCTTGACATCGATAAAGCTTAATTTTGTTTTCGTT GTGCGTGGTATTTGTAATTTAGTACATTCTCTGGACTCTGGAGCATCCTTGAGATAAAGCCTGTATTGTGTT TAAGTTTGTTTTAGACAGTAGCAAAACTAATCAAACTGTCTTTGCGCCATTCAAATCTTACTCGGTAAAATA AAAAGTTTTACTTTTAGTATTTGGACCTAA

Table S3: Amino acid percent-identity matrix among sacred lotus *O*-methyltransferase (OMT) candidates and functionally characterized OMTs from BIA-accumulating species. OMTs sharing more than 40% amino acid sequence identity are highlighted.

	NnOMT1	NnOMT2	NnOMT3	NnOMT4	NnOMT5
NnOMT2	84				
NnOMT3	83	84			
NnOMT4	81	77	74		
NnOMT5	46	44	44	45	
Tf6OMT	69	64	62	62	46
Ps6OMT	63	58	57	59	46
Cc6OMT1	43	43	41	42	43
Cc6OMT2	69	64	63	62	46
Cj6OMT	69	64	63	62	46
GfOMT2	69	64	63	63	47
TtOMT1	39	39	37	35	36
TtOMT2	38	38	36	34	36
Cj4'OMT	54	51	52	50	45
Ec4'OMT	52	50	51	50	43
GfOMT1	53	51	51	50	43
Ps4'OMT2	52	50	49	49	41
PsSOMT2	41	39	38	40	42
PsSOMT3	59	53	52	54	43
Ct7OMT	44	43	42	39	38
Ec7OMT	43	43	42	42	41
Ps7OMT	40	41	40	38	41
PsN7OMT	55	53	50	51	44
CjCoOMT	42	40	39	40	45
CjSOMT	34	33	32	31	27
CtSOMT	34	34	33	31	27
EcSOMT	41	41	39	39	42
GfOMT6	35	35	34	32	27
GfOMT7	37	37	35	33	35
PsSOMT1	33	32	32	29	30

Table S4: Substrate range for recombinant NnOMT candidates. Substrate conversion represents the mean ± standard deviation of three independent replicates. Structures corresponding to tested aporphine, protoberberine and morphinan substrates are shown. Nd, not detected.

Class	Alkaloid	Substrate conversion (nmol min^{-1} mg^{-1} protein)				
		NnOMT1	NnOMT2	NnOMT3	NnOMT4	NnOMT5
1-Benzylisoquinoline	(*R*,*S*)-Norcoclaurine	0.30 ± 0.02	nd	nd	nd	0.22 ± 0.03
	(*S*)-Norlaudanosoline	0.38 ± 0.10	nd	nd	nd	0.05 ± 0.02
	(*R*)-Norlaudanosoline	0.30 ± 0.08	nd	nd	nd	nd
	(*S*)-Coclaurine	nd	nd	nd	nd	0.57 ± 0.04
	(*S*)-*N*-Methylcoclaurine	nd	nd	nd	nd	0.68 ± 0.01
	(*S*)-Reticuline	nd	nd	nd	nd	0.53 ± 0.05
	(*R*)-Reticuline	nd	nd	nd	nd	nd
	(*R*)-Armepavine	nd	nd	nd	nd	nd
Aporphine	Boldine	nd	nd	nd	nd	nd
	(+)-Bulbocapnine	nd	nd	nd	nd	nd
	(+)-Isocorydine	nd	nd	nd	nd	nd
Protoberberine	(*S*)-Scoulerine	nd	nd	nd	nd	nd
	(13*S*,14*R*)-1,13-Dihydroxy *N*-methylcanadine	nd	nd	nd	nd	nd
Morphinan	Codeine	nd	nd	nd	nd	nd
	Morphine	nd	nd	nd	nd	nd

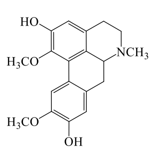
Boldine

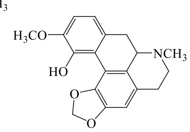
(+)-Bulbocapnine

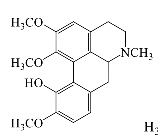
(+)-Isocorydine

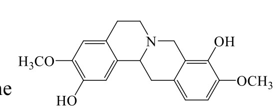
(*S*)-Scoulerine

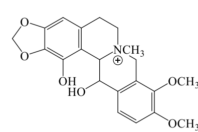
(13*S*,14*R*)-1,13-Dihydroxy *N*-methylcanadine

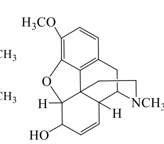
Codeine

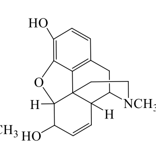
Morphine

Table S5: Alkaloid content in different organs and tissues of two sacred lotus varieties. FL, folded leaf; UL, unfolded leaf; Rh, rhizome; Ro, roots; E, embryos; DW, dry weight.

Lotus variety	Organ	Alkaloid content (nmol g^{-1} DW)			
		Norcoclaurine	Coclaurine	*N*-methylcoclaurine	Armepavine
Pink	FL	0.511 ± 0.011	0.106 ± 0.006	1.696 ± 0.050	0.184 ± 0.000
	UL	0.590 ± 0.001	0.152 ± 0.000	0.795 ± 0.018	0.082 ± 0.000
	Rh	0.067 ± 0.002	0.018 ± 0.000	0.481 ± 0.005	0.030 ± 0.000
	Ro	0.000 ± 0.000	0.004 ± 0.000	0.038 ± 0.001	0.001 ± 0.000
	E	0.143 ± 0.003	0.093 ± 0.040	0.018 ± 0.003	0.000 ± 0.000
White	FL	1.396 ± 0.015	0.255 ± 0.008	1.122 ± 0.020	0.155 ± 0.000
	UL	1.107 ± 0.058	0.346 ± 0.020	0.460 ± 0.016	0.084 ± 0.000
	Rh	0.018 ± 0.001	0.011 ± 0.000	0.241 ± 0.001	0.019 ± 0.000
	Ro	0.001 ± 0.000	0.036 ± 0.001	0.017 ± 0.001	0.000 ± 0.000
	E	0.195 ± 0.009	0.055 ± 0.036	0.184 ± 0.016	0.149 ± 0.001

Table S6: *O*-methyltransferase activity in different organs and tissues of two sacred lotus varieties. FL, folded leaf; UL, unfolded leaf; Rh, rhizome; Ro, roots; E, embryos.

Lotus variety	Organ	Specific activity (nmol min^{-1} mg^{-1} protein)		
		6OMT	7OMT	4'OMT
Pink	FL	2.78 ± 0.44	0.44 ± 0.04	0.00 ± 0.00
	UL	0.00 ± 0.00	1.21 ± 0.09	0.00 ± 0.00
	Rh	0.11 ± 0.04	0.31± 0.06	0.00 ± 0.00
	Ro	0.00 ± 0.00	0.19 ± 0.04	0.00 ± 0.00
	E	1.59 ± 0.09	0.77 ± 0.11	0.00 ± 0.00
White	FL	3.96 ± 0.85	0.79 ± 0.13	0.00 ± 0.00
	UL	0.21 ± 0.04	1.72 ± 0.20	0.00 ± 0.00
	Rh	0.12 ± 0.05	0.21 ± 0.02	0.00 ± 0.00
	Ro	0.10 ± 0.01	0.49 ± 0.02	0.00 ± 0.00
	E	3.86 ± 0.37	0.80 ± 0.06	0.00 ± 0.00

Table S7: *OMT* transcript levels in different organs and tissues of two sacred lotus varieties. FL, folded leaf; UL, unfolded leaf; Rh, rhizome; Ro, roots; E, embryos.

Lotus variety	Organ	Mean relative transcript abundance ($2^{-\Delta\Delta CT}$)				
		NnOMT1	NnOMT2	NnOMT3	NnOMT4	NnOMT5
Pink	FL	8804	1153	2205	1568	11743
	UL	1227	85	222	359	11154
	Rh	3792	425	1295	721	7203
	Ro	848	74	141	214	4116
	E	1323	957	1963	1292	1118
White	FL	11752	1378	662	3089	12299
	UL	5579	414	12	586	10747
	Rh	10	1	1	102	4090
	Ro	1808	173	152	406	3188
	E	688	1034	494	399	1037

Table S8: Primers used to **(a)** amplify sacred lotus *OMT* candidate genes, **(b)** perform quantitative real-time PCR (qRT-PCR), and **(c)** linearize the pRSET-A vector. For NnOMT cDNA cloning, a 5'-3' sequence (GGT TCT CAT CAT CAT CAT CAT CAT [FW] or TCC ACC AGT CAT GCT AGC CAT ACC [RV]) was added to each OMT FW or RV primer, respectively, showed in **(a)**.

	Gene	Forward primer (5'-3')	Reverse primer (5'-3')
(a)	NnOMT1	ATG GAA ATT CAG AAG GAA GGT CAA GC	CTA ATA AGG ATA GGC CAC AAT TAC AGA TTG AAC G
	NnOMT2	ATG GAA ATT CCG AAG	CTA ATA AGG ATA GGC C
	NnOMT3	ATG GAA ATT CAG AAG GAA GTT CAA GC	CTA ATA AGG ATA GGC CTC AAT TAC AGA TTG AAC G
	NnOMT4	ATG GAA AAT CAG AAG GAA GTT CAA GC	CTA ATA AGG ATA GGC CTC AAT TAC AGA GTA CTC
	NnOMT5	ATG GAG GAG GAC ATG AAA GC	TCA AGG GAA CAC TTC TAT AAT TGA TTC G
(b)	NnOMT1	GGA CAA GAG CAT AGT GTC AAT C	TCC ATA TGC TCC TCC CTA AC
	NnOMT2	GCT ATC TCC ACA CGG TAA GT	CCT CGT CAG TGA TCG CTA ATA
	NnOMT3	CTG GTA CCG TCT CAA GGA TAG	GGA TGA TCA GCC ATG CAT TC
	NnOMT4	GGT GTT AGG GAA GAG CAT ATC G	CTG ATG TGA AGA GCC TGG TAT C
	NnOMT5	CAG TGG GTG GTA AAG AGA GAA G	AGA TAA CAC CCA TCG TTG CA
	Nn*B*-Actin	AGG GAG AAG ATG ACC CAG ATT A	GTT GTT CTA CCA CTG GCG TAT AG
(c)	Vector	GGT ATG GCT AGC ATG ACT	ATG ATG ATG ATG ATG ATG AGA

Table S9: Amino acid sequence of functionally characterized OMTs involved in BIA biosynthesis in the Ranunculales. Enzymes are represented according to their primary reported regiospecificity.

Specie	GenBank ID (abbreviation)	Amino acid sequence	Ref.
		4'OMT	
Coptis japonica	D29812 (Cj4'OMT)	MAFHGKDDVLDIKAQAHVWKIIYGFADSLVLRCAVELGIVDIIDNNNQPMALADLASKLPVSDVN CDNLYRILRYLVKMEILRVEKSDDGQKKYALEPIATLLSRNAKRSMVPMILGMTQKDFMTPWHS MKDGLSDNGTAFEKAMGMTIWEYLEGHPDQSQLFNEGMAGETRLLTSSLISGSRDMFQGIDSLVD VGGGNGTTVKAISDAFPHIKCTLFDLPHVIANSYDLPNIERIGGDMFKSVPSAQAIILKLILHDWND EDSIKILKQCRNAVPKDGGKVIIVDVALDEESDHELSSTRLILDIDMLVNTGGKERTKEVWEKIVKS AGFSGCKIRHIAAIQSVIEVFP	(6)
Eschscholzia californica	AB745041 (Ec4'OMT)	MGLEFNEEVDIKAQAHLWNIIYGFADSLVLRSAVELGIADIIKNNNGSITVSELASKLPISNVNSDNL YRVLRYLVHMGILKETKSTINGGEIKKLYSLEPVGSLLVKDAERNMVPIVLGMTQQDFMIPWHYI KEGLGEGSTAFEKGMGMTLWEYLEGHPEQGHLFNVGMEGETRLLTKTLIESCKDTFEGLSSLVDV GGGNGTTIKAISEAFPHIKCSLYDLPHVVADSHDLPNIEKIPGDIFKFIPNAQAILLKLILHDWSDEDS VKILKKCREAVPQDTGRVIIVDVALEEESEHPLTKTRLVLDVDMLVNTGGRERSEDDWAKLLKLA GFRTHKIRHIAAVQSVIEAFP	(7)
Glaucium flavum	KP176693 (GfOMT1)	MGVSDNKPESQEVDIKAQAHLWNIIYGFADSLVLRCAVEIGIADIIKSNNGSISVTELASKLPITNVN SDNLYRVLRYLVHMGILKEVSDSNEVKLYSLQPVATLLLRDAERSMVPIILGMTQKDFMIPWHFM KEGLGNDTTAFEKGMGMTIWQYLEGHPEQSNLFNEGMAGETRLLTKSLIDGCRDTFEGLTSLCDV GGGNGTTIKGIYDAFPQIKCSVYDLPHVIASSPEHPNIERIPGDMFKSVPSAQAILLKLILHDWTDEE CVNILIKCREAVPKDTGKVIIVDVALEEESQHELTKTRLILDIDMLVNTGGRERSEDDWEKLLKRA GFRGHKIRHIAAIQSVIEAFP	(8)
Papaver somniferum	AY217334 (Ps4'OMT2)	MGSLDAKPAAATQEVSIKDQAQLWNIIYGFADSLVLRCAVEIGIADIIKNNDGAITLAQLAAKLPIT NVSSDYLYRMVRYLVHLNIIEQETCNGGVEKVYSLKPVGTLLLRDAERSMVPMILGMTQKDFMV SWHFMKEGLGNGSTTAFEKGMGMDIWKYLEGNPDQSQLFNEGMAGETRLLTKTLIEDCRDTFQG LDSLVDIGGGNGTTIKAIYEAFPHIKCTLYDLPHVVANSHDLPNIEKVPGDMFKSVPSAQAILLKLIL HDWTDEECVNILKKCKEAIPKETGKVIIVDVALEEESNHELTKTRLILDIDMLVNTGGRERTADDW ENLLKRAGFRSHKIRPIRAIQSVIEAFP	(9)
	Ps4'AOMT MH029292 (PsSOMT2)	MEIHLESQEQEMKYQSQIWNQICGTVDTSVLRCAIQLGIFDAIHNSGKPMITLTELSSIVSSPSSSSIE PCNLYRLVRYLSQMDLISIGECLNEATVSLTGTSKLLLRNQEKSLIDWVLAIXCEMMVVVWHELS SSVSTPADEPPIFQKVHGKNALELAGEFPEWNDLINNAMTSDTSVTKPALIQGCGKILNGVTSLIDV GGGHGATMAYIVEAFPHIKGAVIDLPHVVEAAPERPGVEFISGDIFKSISNADAVLLKYVLHNWED TECVNLLKRCKEAVPADKGKVIIMDLVIDDDDNSILTQAKLSLDLTVMNHGGGRERTKEDWRNLI EMSGFSRHEIIPISAMPSIIVAYP	(10)
	MH029294 (PsSOMT3)	MEVVSKIDQENQAKIWKQIFGFAESLVLKCAVQLEIAETLHNNVKPMSLSELASKLPAQPVNEDRL YRILHFLVHMKLFNKDATTQKYSLAPPAKYLLKGWEKSMVPSILSVTDKDFTAPWNHLGDGLTG NCNAFEKALGKGIRVYMRENPEKDQLFNEGMACDTRLFASALVNECKSIFSDGINTLAGVGRGTG TAVKAISKAFPDIKCTIHDLPEVTSKNSKIPRDVFKSVPSADAIFMKSILHEWNDEECIQILKRCKEAI PKGGKVIIADVVIDMDSTHPYSKSRLAMDLAMMLHTGGKERTEEDWKKLIDAAGFASCKITKLSA LQSVIEAYPH	
		6OMT	
Coptis chinensis	MH165875 (Cc6OMT1)	MQIQNEEQEQDMKSHAQILNHMCGIVDSVVLKCAVELNLFDVISNNKDSKPIALSSLATSPTLVSI KPNNLYRLLRYLVHMNLLTIHVEGNDETFSLTELSKLLLRDQNRSLVDWALAIIDETVIDGWHELS GCCTSPTGPTPFERVHGKSVWELAGENAGMNQVINDAMVSDTILVMPVFVQCCDKLLNGITSMV DIGGGVGMTMSYIVKAFPHIKCTVFDLPHVIASSAQLPGVEMVGGDMFKFIPPADAIFLKFMLHN WHDKECITILKKCKEVIPQDKGKVIILDIVTDQNEQDDDLTRAKMNLDIDMMVTSGGRERTENEW EVLLKLAGFSRHEIIPIMAVQSVIVAYP	(11)
	MH165876 (Cc6OMT2)	MVKKDNLSSQAKLWNFIYGFAESLVLKCAVQLDLANIIHNNGTSMTLSELSSRLPSQPVNEDALY RVMRYLVHMKLFTKASIDGELRYGLAPPAKFLVKGWDKCMVGSILAITDKDFMAPWHYLKDGL AGESGTAFEKALGMNIWGYMAEHPEKNQLFNEAMANDSRLIMSALVKECGNIFNGITTLVDVGG GTGTAVRNIANAFPHIKCTVYDLPHVIADSPGYSEVHCVAGDMFKFIPKADAIMMKCILHDWDDK ECIEILKRCKEAVPIEGGKVIIVDIVLNVQSEHPYTKMRLTLDLDMMLNTGGKERTEEEWKNLIHD AGYKGHKITQITAVQSVIEAYPY	(11)
Coptis japonica	D29811 (Cj6OMT)	MEVKKDNLSSQAKLWNFIYGFAESLVLKCAVQLDLANIIHNSGTSMTLSELSSRLPSQPVNEDALY RVMRYLVHMKLFTKASIDGELRYGLAPPAKYLVKGWDKCMVGSILAITDKDFMAPWHYLKDGL SGESGTAFEKALGTNIWGYMAEHPEKNQLFNEAMANDSRLIMSALVKECGNIFNGITTLVDVGGG TGTAVRNIANAFPHIKCTVYDLPHVIADSPGYSEVHCVAGDMFKFIPKADAIMMKCILHDWDDKE CIEILKRCKEAVPVKGGKVIIVDIVLNVQSEHPYTKMRLTLDLDMMLNTGGKERTEEEWKKLIHD AGYKGHKITQITAVQSVIEAYPY	(6)

Glaucium flavum	KP176694 (GfOMT2)	MEATKSDQANQANIWKLIYGFAESLVLKCAIQLEIADTIHNHGEPMSLSELASKLPVQPVNSDRLY RVMRYLVHMKLFNKEKTSINGEFKYSLAPPAKFLIKGWEKSMVASILAINDKDFLAPWHHLKDGL SGDCDAFEKALGKSIWVYMSENPEKNQLFNEAMACDTRLVTSALVNDCQSVFKGINTLVDVGGG TGTAVKAISKAFPHIKCSIYDLPHVIADSPEIPNVVKIEGDMFKAIPSADAILMKCILHDWNDDECIQ ILKKCKEAVPQEGGKVIIVDVVLNMDLTHPYSKIRLTLDLDMMLNTGGKERTVEEWKKLIDAAGF ASFKITEISAVQSVIEAFPY	(8)
Papaver somniferum	AY217335 (Ps6OMT)	METVSKIDQQNQAKIWKQIYGFAESLVLKCAVQLEIAETLHNNVKPMSLSELASKLPVAQPVNED RLFRIMRYLVHMELFKIDATTQKYSLAPPAKYLLRGWEKSMVDSILCINDKDFLAPWHHLGDGLT GNCDAFEKALGKSIWVYMSVNPEKNQLFNAAMACDTRLVTSALANECKSIFSDGISTLVDVGGGT GTAVKAISKAFPDIKCTIYDLPHVIADSXEIPNITKISGDMFKSIPSADAIFMKCILHDWNDDECIQIL KRCKEALPKGGKVIIVDVVIDMDSTHPYAKIRLTLDLDMMLNTGGKERTKEEWKTLFDAAGFAS HKVTQISAVQSVIEAYPY	(9)
Thalictrum flavum	AY610507 (Tf6OMT)	MEMINKENLSSQAKLWNFIYGFADSLVLKSAVQLDLANIIHNHGSPMTLSELSLHLPSQPVNQDAL YRVLRYLVHMKLFTKSSIDGELRYGLAPPAKFLVKGWDKCMLGAILTITDKDFMAPWHYLKEGIL NDGSTSTAFEKALGTNIWDYMAEHPEKNQLFNEGMANDTRLIMSALVKECSSMFDGITTIVDVGG GTGTAVRNIAKAFPHIKCTVYDLPHVIADSPGYTEINSIQGDMFKYIPNADAIMMKCILHDWDDKE CIEILKRCKDAVPRDGGKVIIIDIILDVKSEHPYTKMRLTLDLDMMLNTGGKERTEEEWKKLIHDA GYKGYKITHISAVQSVIEAYPY	(12)
Thalictrum tuberosum	AF064693 (TtOMT1)	MGSTENNHNLTPAEEEEEEAYLHAMQLASASVLPMVLKAAIELDVLEIIAKAGKGAYVAPSEIAS QLSTSNSQAPTVLDRMLRLLASYKVLTCNLRNLEDGGVERLYGLAPVCKFLVKNEDGVSMAPLV LMNQDKVLMESWYHLKDAVLDGGIPFNKAYGMTAFEYHGTDPRFNKVFNRGMADHSTITMKKL LELYKGFEGLKSVVDVGGGTGATVNMIVTKHPTIKGINFDLPHVIDDAPAYPGVEHIGGDMFVSV PKGDAIFMKWILHDWSDEHSVKFLKNCYESIPADGKVIIVESVLPVFPETNLAAHTCFQLDNIMLA HNPGGKERTEKDFKALSVKAGFTGFKVVCGAFGSWVMEFCK	(13)
	AF064694 (TtOMT2)	MGSTQKNHNLTPEEEEEACLHAMQLASASVLPMVLKAAIELSVLEIIAKAGQGAYVAPTEIASQLS TSNSQAPIILDRILRLLASYKVLTCNLRTLEDGGVERLYGLAPVCKFLVKNEDGVSIAPLVLMNQD KVLMESWYHLKDAVLDGGIPFNKAYGMTAFEYHGTDPRFNKVFNRGMADHSTITMKKLLELYK GFEGLKSVVDVGGGTGATINMIVTKHPTIKGINFDLPHVIDDAPAYPGVEHIGGDMFVSVPKGDAI FMKWILHDWSDEHSVKFLKNCYESIPADGKVIIVESILPVYPETNLASNACFQLDNIMLAHNPGGK ERTEKDFEALSAKAGFTGFKIVCGAFGSWVMEFCK	(13)
		7OMT	
Coptis teeta	MH165877 (Ct7OMT)	METILQGQQNITKLLFAFADTMALKCVVELRIADIINSHGLPISLSEIAAGIQSTSSSSSPPNINYLFRI MRLLVRKGVFSSHAPNQNEETLYGLTNSSKWLLRDANFSMTPIIQALTHHCSMDSFHKLNKCVEE GGYAFAKANGCEIWEFASMNPEFNRLFNSAMASTSKIAVDAILSGYKNGFDGLRSLVDVGGGTGT LIGEIVKAYPHLTGTNFDLPHVVATAPEHTGVVHVGGDMFVEIPHADAIILKWILHDWNDEDCVKI LKNCHKAIANRGVKVIIVEIVLQPDGVAPLDETRLIFDLSMIAHSSGGKERTETEWEKLLRDGGFSR HRIIQIPDVTSIIEAYP	(11)
Eschscholzia californica	AB232153 (Ec7OMT)	MDEEIILGQADICKYMYGFVDSMTLRCVVELGIPDIIHSHGRPITLTEILNGIPNLSSSFDINYLQGIM TILVRRRVFAVHKFDPKDGTNLTEIRYGLTPSSKCLLKDSKFNLAPFVLLETHPWITDPWNYLGKC VQEGGSGFVKAHGSDVFKFGSDHPEFFKLFYDGMECSTKVLVQVVLDKYQQVFKDVKSIVDVGG GTGMMISEIVKNHPHIKGINFDLPHVVAEAPDYPGVEHVGGDMFVEIPQADAITMKGILHDWNDD ACVKILENCKKAIPKNGKVIIIDCVLNPDGDDLFDDIKVVSDLGMRVHCSDGKERTEAEWEKLLK KGGFPRYKITHVVTVQSMIEAYPE	(14)
Papaver somniferum	AY268893 (Ps7OMT)	MDTAEERLKGQAEIWEHMFAFVDSMALKCAVELGIPDIINSHGRPVTISEIVDSLKTNTPSSSPNID YLTRIMRLLVHKRLFTSELHQESNQLLYNLTRSSKWLLKDSKFNLSPLVLWETNPILLKPWQYLGK CAQEKSSPFERAHGCEIWDLALADPKFNNFLNGAMQCSTTTIINEMLLEYKDGFSGIAGSLVDVGG GTGSIIAEIVKAHPHIQGINFDLPHVVATAAEFPGVKHVGGDMFVDIPEADAVIMKWILHDWSDED CTIILKNCYRAIRKKKNGKVIIVDCVLRPDGNDLFDKMGLIFDVLMMAHTTAGKERTEAEWKILL NNAGFPRYNVIRTPAFPCIIEAFPE	(15)
	FJ156103 (PsN7OMT)	MEVVSQIDQENQAIIWKQIYGFSESLLLKCAVQCEIAETIHNHGTPMSILELAAKLPIDQPVNIDRLY RVMRYLVHQKLFNKEVISTLNGGTVQVTEKYWLAPPAKYLIRGSQQSMVPSVLGIIDEDMFAPW HILKDSLTGECNIFETALGKSISVYMSENPEMNQISNGAMAFDSGLVTSHLVNECKSVFGDEIKTLV DVGGGTGTALRAISKAFPNIKCTLFDLPHVIADSPEIPTITKVSGDMFKSIPSADAIFMKNILHDWND DECIQILKRCKDVVSAGGKLIMVEMVLDEDSFHPYSKLRLTSDIDMMVNNGGKERTEKEWEKLF DAAGFASCKFTQMSVGFAAQSIIEVY	(16)
		CoOMT	
Coptis japonica	AB073908 (CjCoOMT)	MDTPNTFQNDDEIKAQAQVWKHMFGFAETIMLRSTVSLGIPDIIHNNGPVTLSQLVTHLPLKSTSID RFHHFMRYLVHMQLFTISTDQITKEDKYELTPASKLLVHGHQKSLAPYVMLQTHPEEFSVWSHVI NVLDGKKPYWESNDTSMYEKTEGDPEINEILNDAMTSHSTFMLPALVSGLMKENVLDGVASIVD VGGNSGVVAKGIVDAFPHVKCSVMDLNHVIERVIKNPKLDYVAGDMFTSIPNADAILLKSTLHNY EDDDCIKILNIAKEALPSTGGKVILVEIVVDTENLPLFTSARLSMGMDMMLMSGKERTKKEWEDL LRKANFTSHQVIPIMAIESIIVAYS	(17)

SOMT			
Coptis japonica	D29809 (CjSOMT)	MCTSLSELKCPVFSTKRKLLLEFALRTSVDMAAQEGVNYLSGLGLSRLICLPMALRAAIELNVFEII SQAGPDAQLSPSDIVAKIPTKNPSAAISLDRILRMLGASSILSVSTTKSGRVYGLNEESRCLVASEDK VSVVPMLLFTSDKAVVESFYNIKDVVLEEGVIPFDRTHGMDFFQYAGKEERVNKSFNQAMGAGS TIAFDEVFKVYKGFDNLKELVDVGGGIGTSLSNIVAKHPHIRGINFELPHVIGDAPDYPGVEHVPGD MFEGVPNAQNILLKWVLHDWDDDRSIKILKNCWKALPENGTVIVIEFVLPQVLGNNAESFNALTP DLLMMALNPGGKERTTIEFDGLAKAAGFAETKFFPISQGLHVMEFHKINC	(18)
Coptis teeta	MH165874 (CtSOMT)	MAAQEGVNYLSGLGLSRLICLPMALRAAIELNVFEIISKAGPDAQLSPSDIVAKIATKNPSAAISLDR ILRMLGASSILSVSTTKSGRVYGLNEESRCLVASEDKVSVVPMLLFTSDKAVVESFYNIKDVVLEE GVIPFDRTHGMDFFQYAGKEQRVNKSFNQAMGAGSTIAFDEVFEVYKGFNNLKELVDVGGGIGT SLSNIVAKYPHIRGINFELPHVIGDAPDYPGVEHVPGDMFEGVPNAQNILLKWVLHDWDDDRSIKI LKNCWKALPENGTVIVIEFVLPQVLGNNAESFNALTPDLLMMALNPGGKERTTIEFDGLAKAAGF AETKFFPISQGLHVMEFHKINC	(11)
Eschscholzia californica	LC171865 (EcSOMT)	MEKGKLEVGEEMELQGQADICKLMLAFIDSMALKCAVELGIPDIIHSQGQPITLSEIINGIPNLSPSF DINYLFRIMRLLVRNRVFSAYEPDLKDGSSGTKTLYGLTPSSKWLVKDSKISLAPLVLAENHPWLL DPWHYLGKCVQEGGFAFAKAHGSEIWKFGSENPEFNKLFSVGMACSSTLVVDAILDDYHEGFGD LESIVDVGGAIGTLINEIVKKYPHIRGTNFDLPHVVAEALENPGVAHVGGDMFVEIPSADAVILKW VLHDWNDEDCVKILKNCNKAISNKGKLIIIECVLKPDGEGLFDGLGLAFDLLMIAHSSGGRERTEA EWKKLLKAGGFSRYKITPIKGIPSIIEAYPDI	(19)
Glaucium flavum	KP176698 (GfOMT6)	METKGEARMNSCYISEAGHLGRLICLPMALRAAVELNVFNIISEFGPGAQLSSRDLVAKIPTTNPNA HVYLERILRLLAASSFLSVSTRTSSSPESITNTNGHHNGDTNGVVNHDNEKVTERVYGLTKESHCL VPRKDDGVSLVPMLMFVADKIVVESFYNLKEVVLQEGRVPFDMTHGASIFEYAGKDPRMNKVFN EAMGDFSVIAFDEVLKVYNGFLDMKELVDVGGGIGTSLSNIVTKYPFIRGINFDLSHVISSAPNYTG VEHVAGDMFEELPKAQNILLKWVLHDWDDKQCLKLLKTCWNSLPAEGGKVIVIEFVVPSKIADN PESYNALTPDLLMMALNPGGKERTLLEFYDLANAAGFAKAKPFPISEGLHVIEFHK	(8)
	KP176699 (GfOMT7)	MGSTQDQFKPTPIEEEEEACMYAMQLASASVPVMVLKAAVELNVLEIIAKHGPGAQISASAIAAHI PNIKNPNAPVMLDRMLRLLASYKILTCTVKDLDDQGLVQQRLYGLALVCKFLVKNEDGCSMAPL LLMNQDKVFLESWYHLKDAVLDGGIPFNKAYGMNAFEYQGADPRFNKIFNRGMSDHTTITMKKI LETYKGFEGLTSLVDVGGGIGVTVDMIVSKYPSIKGINFDLPHVIKDAPSYPGVEHVGGDMFASIPK GDAIFMKWILHDWSDEHGIKILKNCYEALPDHGKVILVECIIPPYPETSLAGLGVFHVDNIMLAHNP GGKERTEKEFEALAKGTGFAGFRVICSAFNTWIMEFSKN	(8)
Papaver somniferum	JN185323 (SOMT1)	MATNGEIFNTYGHNRQTATVTKITASNESSNGVCYLSETANLGKLICIPMALRAAMELNVFQLISK FGTDAKVSASEIASKMPNAKNNPEAAMYLDRILRLLGASSILSVSTTKKSINRGGDDVVVHEKLYG LTNSSCCLVPRQEDGVSLVEELLFTSDKVVVDSFFKLKCVVEEKDSVPFEVAHGAKIFEYAATEPR MNQVFNDGMAVFSIVVFEAVFRFYDGFLDMKELLDVGGGIGTSVSKIVAKYPLIRGVNFDLPHVIS VAPQYPGVEHVAGDMFEEVPKGQNMLLKWVLHDWGDERCVKLLKNCWNSLPVGGKVLIIEFVL PNELGNNAESFNALIPDLLLMALNPGGKERTISEYDDLGKAAGFIKTIPIPISNGLHVIEFHK	(20)

References

1. Robin, A. Y., Giustini, C., Graindorge, M., Matringe, M., and Dumas, R. (2016) Crystal structure of norcoclaurine-6-O-methyltransferase, a key rate-limiting step in the synthesis of benzylisoquinoline alkaloids. *Plant J.* 87, 641-653
2. Zhang, L., Shi, J., Tang, J., Cheng, Z., Lu, X., Kong, Y., and Wu, T. (2017) Direct coupling of thin-layer chromatography-bioautography with electrostatic field induced spray ionization-mass spectrometry for separation and identification of lipase inhibitors in lotus leaves. *Anal Chim Acta.* 967, 52-58
3. Lin, Z., Yang, R., Guan, Z., Chen, A., and Li, W. (2014) Ultra-performance LC separation and quadrupole time-of-flight MS identification of major alkaloids in Plumula Nelumbinis. *Phytochem Anal.* 25, 485-494
4. Deng, X., Zhu, L., Fang, T., Vimolmangkang, S., Yang, D., Ogutu, C., Liu, Y., and Han, Y. (2016) Analysis of Isoquinoline Alkaloid Composition and Wound-Induced Variation in Nelumbo Using HPLC-MS/MS. *J Agric Food Chem.* 64, 1130-1136
5. Luo, X., Chen, B., Liu, J., and Yao, S. (2005) Simultaneous analysis of *N*-nornuciferine, *O*-nornuciferine, nuciferine, and roemerine in leaves of *Nelumbo nucifera* Gaertn by high-performance liquid chromatography–photodiode array detection–electrospray mass spectrometry. *Analytica Chimica Acta.* 538, 129-133
6. Morishige, T., Tsujita, T., Yamada, Y., and Sato, F. (2000) Molecular characterization of the S-adenosyl-L-methionine:3'-hydroxy-N-methylcoclaurine 4'-O-methyltransferase involved in isoquinoline alkaloid biosynthesis in Coptis japonica. *J Biol Chem.* 275, 23398-23405
7. Inui, T., Tamura, K., Fujii, N., Morishige, T., and Sato, F. (2007) Overexpression of Coptis japonica norcoclaurine 6-O-methyltransferase overcomes the rate-limiting step in Benzylisoquinoline alkaloid biosynthesis in cultured Eschscholzia californica. *Plant Cell Physiol.* 48, 252-262
8. Chang, L., Hagel, J. M., and Facchini, P. J. (2015) Isolation and Characterization of O-methyltransferases Involved in the Biosynthesis of Glaucine in Glaucium flavum. *Plant Physiol.* 169, 1127-1140
9. Facchini, P. J., and Park, S. U. (2003) Developmental and inducible accumulation of gene transcripts involved in alkaloid biosynthesis in opium poppy. *Phytochemistry.* 64, 177-186
10. Park, M. R., Chen, X., Lang, D. E., Ng, K. K. S., and Facchini, P. J. (2018) Heterodimeric O-methyltransferases involved in the biosynthesis of noscapine in opium poppy. *Plant J.* 95, 252-267
11. He, S. M., Liang, Y. L., Cong, K., Chen, G., Zhao, X., Zhao, Q. M., Zhang, J. J., Wang, X., Dong, Y., Yang, J. L., Zhang, G. H., Qian, Z. L., Fan, W., and Yang, S. C. (2018) Identification and Characterization of Genes Involved in Benzylisoquinoline Alkaloid Biosynthesis in Coptis Species. *Front Plant Sci.* 9, 731
12. Samanani, N., Park, S. U., and Facchini, P. J. (2005) Cell type-specific localization of transcripts encoding nine consecutive enzymes involved in protoberberine alkaloid biosynthesis. *Plant Cell.* 17, 915-926
13. Frick, S., and Kutchan, T. M. (1999) Molecular cloning and functional expression of O-methyltransferases common to isoquinoline alkaloid and phenylpropanoid biosynthesis. *Plant J.* 17, 329-339
14. Fujii, N., Inui, T., Iwasa, K., Morishige, T., and Sato, F. (2007) Knockdown of berberine bridge enzyme by RNAi accumulates (S)-reticuline and activates a silent pathway in cultured California poppy cells. *Transgenic Res.* 16, 363-375
15. Ounaroon, A., Decker, G., Schmidt, J., Lottspeich, F., and Kutchan, T. M. (2003) (R,S)-Reticuline 7-O-methyltransferase and (R,S)-norcoclaurine 6-O-methyltransferase of Papaver somniferum - cDNA cloning and characterization of methyl transfer enzymes of alkaloid biosynthesis in opium poppy. *Plant J.* 36, 808-819
16. Pienkny, S., Brandt, W., Schmidt, J., Kramell, R., and Ziegler, J. (2009) Functional characterization of a novel benzylisoquinoline O-methyltransferase suggests its involvement in papaverine biosynthesis in opium poppy (Papaver somniferum L). *Plant J.* 60, 56-67
17. Morishige, T., Dubouzet, E., Choi, K. B., Yazaki, K., and Sato, F. (2002) Molecular cloning of columbamine O-methyltransferase from cultured Coptis japonica cells. *Eur J Biochem.* 269, 5659-5667
18. Takeshita, N., Fujiwara, H., Mimura, H., Fitchen, J. H., Yamada, Y., and Sato, F. (1995) Molecular cloning and characterization of S-adenosyl-L-methionine:scoulerine-9-O-methyltransferase from cultured cells of Coptis japonica. *Plant Cell Physiol.* 36, 29-36
19. Purwanto, R., Hori, K., Yamada, Y., and Sato, F. (2017) Unraveling Additional O-Methylation Steps in Benzylisoquinoline Alkaloid Biosynthesis in California Poppy (Eschscholzia californica). *Plant Cell Physiol.* 58, 1528-1540
20. Desgagne-Penix, I., and Facchini, P. J. (2012) Systematic silencing of benzylisoquinoline alkaloid biosynthetic genes reveals the major route to papaverine in opium poppy. *Plant J.* 72, 331-344